

УДК 539.12.01

## ON KINEMATICAL AND DYNAMICAL FACTORS IN EXPERIMENTAL OBSERVATION OF DEUTERON-STRIPPING THRESHOLD EFFECTS

*H. Comisel, C. Hategan*

Institute of Atomic Physics, Bucharest, Romania

In this work we discuss kinematical and dynamical factors which could result in inhibition of the deuteron-stripping threshold effects. These effects are determined both by the reaction mechanism of  $(d, p)$  background reaction and by the strength function of the  $3p$ -wave neutron single-particle threshold resonance. The inhibiting factors related to the reaction background depend on its multistep components (small spectroscopic factor),  $Q$ -value and transferred angular momentum. The two spin-orbit components of the  $p$ -wave neutron zero-energy resonance yield different values for quantum kinematical factors, threshold compression factors and threshold anomaly terms; they result in a diminution of the  $3p_{1/2}$  threshold effect as compared to the  $3p_{3/2}$  one.

Обсуждаются кинематические и динамические факторы, которые приводят к подавлению пороговых эффектов дейтрон-стриппинговых реакций. Эти эффекты определяются как механизмом фоновой реакции  $(d, p)$ , так и силовой функцией  $3p$ -волны нейтронного одночастичного порогового резонанса. Подавляющие факторы, связанные с фоном реакции, зависят от его многошаговых компонент (малый спектроскопический фактор), величины  $Q$  и переданного углового момента. Две спин-орбитальные компоненты  $p$ -волны нейтронного резонанса с нулевой энергией дают различные значения для квантовых кинематических факторов, факторов порогового сжатия и пороговых аномальных слагаемых; они приводят к уменьшению  $3p_{1/2}$ -порогового эффекта по сравнению с  $3p_{3/2}$ -пороговым эффектом.

### INTRODUCTION

The threshold effects are directly related to reaction dynamics; e.g., the potential scattering is implied in the Wigner–Baz cusp. The  $p$ -wave threshold effect is related to quasisonant scattering, i.e., a zero-energy neutron threshold state of large spectroscopic amplitude and a strong coupling of neutron threshold channel to open observed one (see Ref. [1]). The spectroscopic quantity defining single-particle state, i.e., its overlap to nucleus actual states, is Neutron Strength Function (NSF). The relationship between  $p$ -wave threshold anomaly and  $3p$  NSF has been recently studied [2, 3]. The strengths of the threshold anomalies observed in deuteron-stripping reactions on  $A \approx 90$  mass target nuclei were evaluated by means of different methods, empirical and computational, and related to the experimental data on  $3p$  NSF. The reaction cross sections were derived, according to computational procedures, by using DWBA formalism and Lane's phenomenologic model for deuteron-stripping threshold anomaly [4]. The mass dependence for strengths of the deuteron-stripping threshold anomaly has been correlated with that of the  $3p$  NSF data in  $80 \leq A \leq 107$  mass range.

This work is complementary to previous ones [2, 3]. Once the anomaly parameters are obtained, a reversed method has been used, by considering the spin-orbit splitting of

$3p$  NSF [5,6]. The two peaks of the  $3p$  NSF are located about  $A \approx 95$  for the  $3p_{3/2}$  component and about  $A \approx 110$  for the  $3p_{1/2}$  one. The deuteron-stripping threshold anomaly strengths have been evaluated and then fitted by using a Lorentzian function in order to follow the mass dependence of the  $3p$  NSF spin-orbit components (see Fig. 1). At a first sight, the result is quite surprising because the large values of  $3p_{1/2}$  NSF around  $A \approx 110$  mass number did provide, according to experimental evidence [7], a weak threshold effect in the cross section for  $^{106}\text{Cd}(d,p)^{107}\text{Cd}$  stripping reaction.

The conclusions of Refs. [2,3] did emphasize the crucial role of  $3p$  NSF in producing the deuteron-stripping threshold anomaly. Weak threshold effects reported in the literature beyond the  $A \approx 110$  mass region suggests a poor presence of  $3p_{1/2}$  NSF. However, the latest studies [6] on  $3p$  NSF spin-orbit splitting reveal the contrary (see experimental data of NSF in Fig. 1). The  $3p_{1/2}$  NSF seems to have similar amplitudes as that of  $3p_{3/2}$  component.

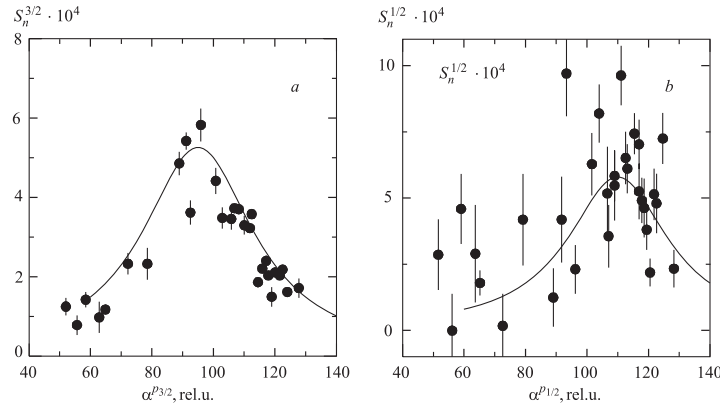


Fig. 1. The mass dependence of the experimental  $3p$ -wave neutron strength function  $S_n$  ( $\bullet$ ) and of the threshold anomaly strength parameters  $\alpha$  (solid curves) derived within a Lorentzian distribution for the: a)  $p_{3/2}$  spin orbit component; b)  $p_{1/2}$  spin orbit component

The factors which could inhibit the contribution of  $3p_{1/2}$ -wave to the deuteron-stripping threshold anomaly are studied in this paper. Some physical aspects concerning the manifestation of the threshold anomalies in deuteron-stripping reactions are discussed in Sec. 1. A numerical experiment has been realized for a better understanding of the interplay between Lane anomalous and DWBA background terms used to describe the threshold effects. In Sec. 2, a numerical prediction of the anomaly for  $A \sim 110$  mass region targets is performed by using the mass dependence of Lane threshold strength parameters ( $\alpha^{p_{3/2}}$  and  $\alpha^{p_{1/2}}$ ) from Fig. 1; the predicted threshold effects will be compared with those reported for  $A \sim 90$  mass region.

## 1. ON DIFFERENT MANIFESTATION OF THE DEUTERON-STRIPPING THRESHOLD ANOMALY FOR $A \sim 90$ AND $A \sim 110$ MASS TARGET NUCLEI

The threshold effect consists of interference between the nonresonant background and the anomalous threshold term. Characteristics of anomaly should be determined by NSF and

background excitation functions too. The background excitation functions for deuteron-stripping reactions on  $A \sim 100$  mass nuclei do exhibit a peak at deuteron energy  $E_d \approx \frac{3}{5}\Delta_C$  [8]. (The empirical Coulombian shift is  $\Delta_C = -1.03 + 1.45Z/A^{1/3}$  [9].) The interplay between the  $Q$ -value of  $(d, p)$  reaction and Coulombian shift  $\Delta_C$  of neutron analogue state results in energy position of analog  $(d, \bar{n})$  threshold channel with respect to background excitation function's peak. The anomaly could be located either on background peak or on its ascending or descending slopes. The deuteron threshold energy  $E_d^{\text{thr}} = \Delta_C - Q_{dp}$ , measured with respect to background peak, is  $\delta = E_d^{\text{pk}} - E_d^{\text{thr}} = Q_{dp} - \frac{2}{5}\Delta_C$ . The anomaly is quite visible near the excitation function peak [8] ( $|\delta| < 0.4$  MeV;  $Q \approx 5$  MeV) and less discernible on ascending ( $\delta > 0.4$  MeV;  $Q > 6$  MeV) or descending ( $\delta < 0.4$  MeV;  $Q < 4$  MeV) slopes.

The threshold anomaly is related to the neutron threshold single-particle state and to the direct interaction (DI) mechanism of deuteron stripping. The interference of the nonresonant background and the threshold resonance is described in terms of direct ( $T^\beta$ ) and resonant ( $T^\pi$ ) transition amplitude elements. Lane [4] proposed the phenomenological model for deuteron-stripping threshold anomaly with  $T^\beta = T^{\text{DWBA}}$  and

$$T^\pi = \sum_{j_p=1/2,3/2} \frac{\alpha^{j_p} \gamma_W^2}{E_{j_p} - E - (S_1 + iP_1 - b)\gamma_{\pi n}^2 - iW}.$$

Here,  $E_{j_p}$  are the energy positions of the neutron threshold resonance (corresponding to  $b$  boundary conditions at  $a$  channel radius);  $S_1$  and  $P_1$  —  $p$ -wave neutron shift and penetration factors;  $\gamma_{\pi n}^2$  is the reduced width of  $p$ -wave neutron single-particle resonance;  $W$  — neutron single-particle spreading width, while  $\gamma_W^2$  stands for the Wigner unit width.

The observed anomaly in deuteron-stripping cross sections depends, consequently, on the magnitude of the direct reaction background,  $\Delta\sigma \cong \text{Re}(T^{\beta*}T^\pi)$ . The  $(d, p)$  cross section has a smaller DI component at backward angles. If the overlap of the neutron single-particle state over the direct interaction in the open channels is small (i.e., small spectroscopic coefficients of the involved states in exit channel), other competing processes, e.g., multistep ones, come to play a more important role in the reaction process [10]. The threshold anomaly cross section  $\Delta\sigma$  will be less discernible if the multistep contributions to  $(d, p)$  cross section are important. Furthermore, these can mask the anomaly in the case of an energy fluctuant behaviour.

For  $A \approx 90$  mass region, the nuclear shell just comes to enclose at  $A = 90$ ; i.e., a  $2d_{5/2}$  pure neutron single-particle state (spectroscopic factor  $\approx 1$ ) is encountered for  $^{91}\text{Zr}$  ground state. The single-particle character of the residual states in stripping reactions becomes weaker while moving away  $A \approx 90$ . For most g.s. nuclei from  $A \approx 110$  mass region, the  $3s_{1/2}$  subshell will be populated by an  $s$ -wave transferred neutron, but the corresponding spectroscopic factors of such states are, as a rule, small. It is expected, on basis of the above arguments, to get less experimental evidences of  $3p$  threshold anomaly in  $A \approx 110$  mass region, where the  $3p_{1/2}$  NSF lies its largest values.

A numerical experiment was devised (Fig. 2) in order to analyze the contribution of each of the  $\alpha^{p3/2}$  and  $\alpha^{p1/2}$  anomaly strengths to the anomalous reaction cross section. The anomalous transition amplitude is added to the direct reaction one provided the deuteron input waves are related to the proton  $p$ -wave in the exit channel. The most trivial partitions for the

angular momenta in the deuteron channel are obtained for an  $s_{1/2}$ -wave transferred neutron. This choice is in accordance with a lot of deuteron-stripping reactions in the mass range  $110 \leq A \leq 130$ . One obtains two quantum number sets ( $l_d = 1, j_d = 0$ ), ( $l_d = 1, j_d = 1$ ) opening  $p_{1/2}$ -wave proton channel and other two ones ( $l_d = 1, j_d = 1$ ), ( $l_d = 1, j_d = 2$ ) for the  $p_{3/2}$ -wave, respectively. Here, ( $l_d, j_d$ ) denotes the values of the orbital and total deuteron angular momenta in the input channel corresponding to the  $p$ -wave exit one. The  $\alpha$  anomaly parameters were distributed among each of the above allowed quantum number sets with the same amplitude and phase. If spin-orbit couplings of the projectile and ejectile particles are considered, the differential cross section is summed over all the spin orientations [10]. The two most significant terms, corresponding to ( $m_p = -1/2, m_d = 1, m = 1/2$ ) and ( $m_p = 1/2, m_d = 0, m = 1/2$ ) spin projections of proton, deuteron and transferred particle, respectively, have been evaluated for  $^{110}\text{Cd}(d, p)^{111}\text{Cd}$  reaction and represented in Fig. 2.

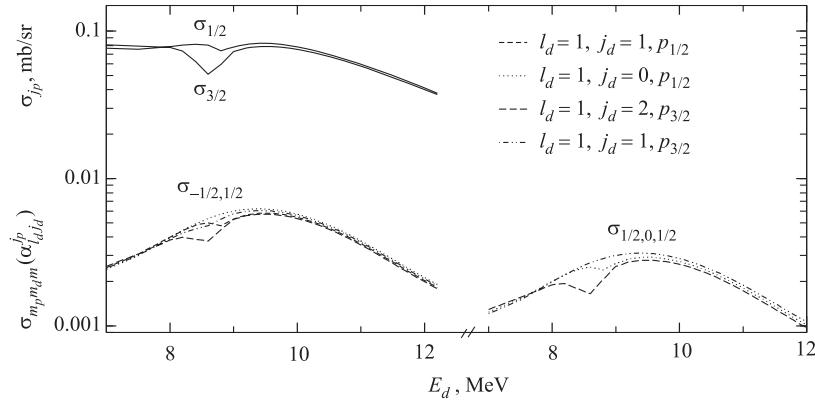


Fig. 2. Numerical test concerning the manifestation of the anomalous effect for  $s_{1/2}$  transferred angular momentum in  $^{110}\text{Cd}(d, p)^{111}\text{Cd}$  differential cross section. Same amplitude and phase for  $\alpha_{(l_d, j_d)}^{p_{3/2}}$  and  $\alpha_{(l_d, j_d)}^{p_{1/2}}$  coefficients corresponding to  $p_{3/2}$ - and  $p_{1/2}$ -wave proton channel do result in different magnitudes of threshold anomaly, see  $\sigma_{3/2}$  and  $\sigma_{1/2}$  solid curves. Such differences are explained by a deeper introspection of DWBA cross-section terms. The two main cross-section terms, labeled by the magnetic numbers of proton, deuteron, and neutron transferred particle, are represented for each allowed deuteron angular momenta (the correspondence with the angular momentum partitions is given in figure's legend). Note that the anomalous dip is strongest and present in both terms (long dashed line) for proton  $p_{3/2}$  wave only

One has to notice the large amplitudes of the anomalous dip for the ( $l_d = 1, j_d = 2$ ) deuteron angular momentum corresponding to  $p_{3/2}$  wave and its occurrence in both considered terms. For the  $p_{1/2}$ -wave case, at least one anomalous contribution vanishes due to the cancellation of a Clebsch–Gordan coefficients product.

The different strengths of the anomalous dip obtained from the above angular momenta partitions in deuteron channel result also from the product of the DWBA «kinematical complex» [10]

$$(2l_p + 1)\sqrt{(2s_d + 1)(2j + 1)(2j_p + 1)(2l_d + 1)}\langle l_p l 0 0 | l_d 0 \rangle \begin{pmatrix} l_p & s_p & j_p \\ l & s & j \\ l_d & s_d & j_d \end{pmatrix}$$

multiplying the radial integrals. Here the quantum numbers  $l$ ,  $s$ ,  $j$  represent the orbital momentum, spin and total spin of the neutron transferred particle. This term could be related to the kinematical factors entering the relationship between the collision matrix derived in total angular momentum coupling scheme and the radial integrals from DWBA approach (see, e.g., [11]).

Similar numerical results have been obtained for  $d_{5/2}$  transferred neutron, specific for  $A \approx 90$  mass region. The deuteron channel with  $(l_d = 3, j_d = 4)$  angular momentum which is related only to  $p_{3/2}$  wave in proton channel has a dominant contribution to the anomalous dip. The  $(l_d = 1, j_d = 2)$  channel analyzed above plays a similar role for the  $s_{1/2}$ -wave transferred angular momentum. As an example, the excitation functions for  $^{106}\text{Cd}(\mathbf{d}, p)^{107}\text{Cd}$  reaction were determined using  $\alpha$  parameters extracted from the derived  $\alpha$ 's mass dependence from Fig. 1 and compared with the experimental data (see Fig. 3). If the  $\alpha^{p_{3/2}}$  strength is set to zero, i.e., the  $3p_{3/2}$  contribution of NSF is canceled, the threshold effect in the cross section becomes very weak, despite the presence of a large  $3p_{1/2}$  NSF component. As a consequence of Yule–Haerberli rule [12], the analyzing power shape is reversed to a resonant form, contrary to the experimental behaviour. The destructive interference between  $p_{3/2}$  and  $p_{1/2}$  terms results in a small anomalous effect when both have been taken into account.

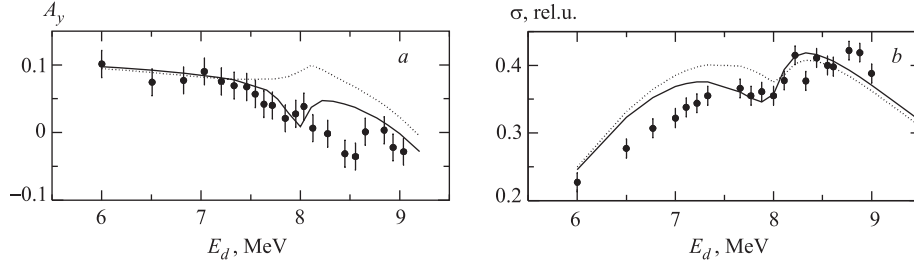


Fig. 3. The experimental excitation functions (filled circles) of analyzing power (a) and differential cross section (b) for  $^{106}\text{Cd}(\mathbf{d}, p)^{107}\text{Cd}$  reaction at  $160^\circ$  scattering angle. The anomalous effect is described using both the  $3p_{3/2}$  and the  $3p_{1/2}$  NSF (solid lines). The dotted lines are obtained for  $3p_{1/2}$  NSF only

A  $d_{3/2}$  transferred angular momentum is also possible for  $A \geq 120$  target nuclei. However, neither  $p_{3/2}$  nor  $p_{1/2}$   $\alpha$ 's strengths can reflect a strong anomalous effect in the excitation functions as does the  $p_{3/2}$  one for the  $d_{5/2}$  or  $s_{1/2}$  transfer deuteron-stripping reactions.

Another factor contributing to the anomalous discrepancies between the  $3/2$  and  $1/2$  spin-orbit terms is the denominator of the Lane anomalous term. As defined in Lane's work, the  $x_j$  parameters fix the spin-orbit energy shift of the resonance,  $x_j = [E_j - (S_1(0) - b)\gamma_{\pi n}^2]/\gamma_W^2$ . It is expected the  $p_{3/2}$  resonance has a positive energy shift below  $A \approx 95$ , while for a  $p_{1/2}$  resonance the energy shift still remains positive up to  $A \approx 110$ . Above these mass limits, the shift coefficients should change their sign. Numerical evaluation of Lane resonant term did evince a decrease of its magnitude when positive values of  $x_{1/2}$  coefficient were getting

larger, according to Lane's estimation ( $x_{1/2} - x_{3/2} = 2$ ,  $-2 \leq \bar{x} \leq 2$ ;  $\bar{x} = 1/2(x_{1/2} + x_{3/2})$ ). For the maximum considered  $x_{1/2} = 3$  value, the amplitude of Lane term for a  $p_{1/2}$ -wave single-particle state is about two times smaller than for the  $p_{3/2}$ -wave correspondent one.

The compression effect due to the rapid variation with energy of the  $S(E)$  shift factor for a neutron single-particle state at zero energy was also reviewed. Lane has evaluated the  $\beta(E)$  compression factor of  $R$ -matrix theory [13],  $\beta(E) = 1/(1 + \gamma_{\pi n}^2 dS/dE)$ , by means of the eigenvalues and eigenfunctions obtained from shell model for the  $3p_{3/2}$  neutron single-particle bound state [4, 14]. The  $\beta(E)$  dependence on single-particle neutron energy was afterwards established by fitting its theoretical value in terms of  $\theta^2$  dimensionless neutron reduced width and  $a$  channel radius defined as fit parameters. Using a similar procedure, our numerical calculations did provide small changes of the above fit parameters when a  $j_p = 1/2$  single-particle neutron state is considered, i.e.,  $\theta^2 = 3.8$ ,  $a = 7.6$  fm [15], while Lane's obtained ones for  $j_p = 3/2$  were  $\theta^2 = 4$ ,  $a = 8$  fm. The cross-section threshold effect becomes weaker if our values for  $\theta^2$  and  $a$  are used.

## 2. NUMERICAL PREDICTIONS

The predictions for the threshold anomaly cross sections in deuteron-stripping reactions, beyond  $A \approx 107$  mass region, were approached by using DWUCK computer code [16], with additional routines for describing the resonant anomalous interaction [17].

In order to evaluate the strength of the deuteron threshold anomaly, DWBA background, corresponding spectroscopic factors and neutron threshold energies have been determined for all «candidate» stripping reactions. We have used, both for protons and for deuterons, the averaged optical model parameters from Refs. [18, 19] or [20]. In case of no experimental evidence of the neutron isobar analogue channel corresponding to the  $p$ -wave proton one, the  $Q$  value of analogue neutron threshold channel was estimated using the empirical method for

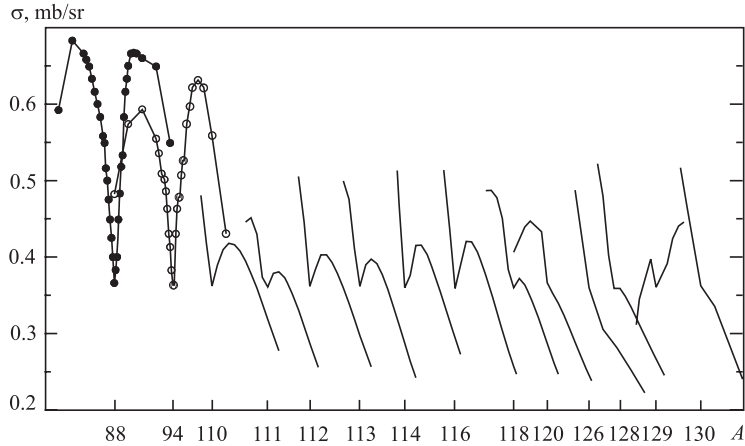


Fig. 4. Experimental differential cross sections for  $^{88}\text{Sr}(d, p)^{89}\text{Sr}$  ( $\bullet$ ) and  $^{94}\text{Zr}(d, p)^{95}\text{Zr}$  ( $\circ$ ) stripping reactions at  $\theta = 160^\circ$  scattering angle. Predicted values for  $100 \leq A \leq 130$  target nuclei have been scaled within the experimental ones. The displayed mass numbers, taken in an ascending order, label the following target nuclei:  $^{88}\text{Sr}$ ,  $^{94}\text{Zr}$ ,  $^{110-114}\text{Cd}$ ,  $^{116}\text{Sn}$ ,  $^{118}\text{Sn}$ ,  $^{120}\text{Sn}$ ,  $^{126}\text{Te}$ ,  $^{128}\text{Te}$ ,  $^{129}\text{Xe}$  and  $^{130}\text{Te}$

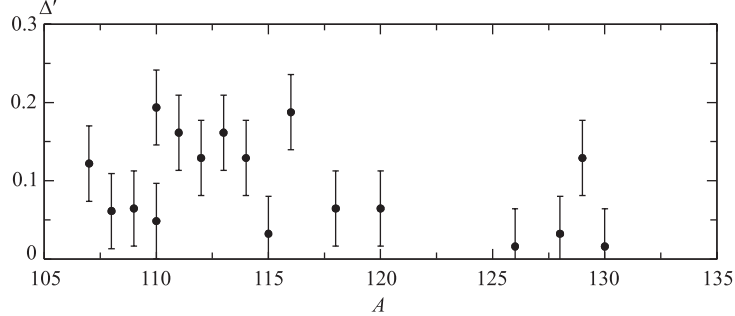


Fig. 5. The  $\Delta' = (\sigma_{\max} - \sigma_{\min})/\sigma_{\min}$  predicted strengths of the deuteron anomaly for target mass nuclei with  $A \geq 106$  determined within the numerical procedure. The values are normalized to the largest observed one from the  $A \approx 90$  mass region,  $^{88}\text{Sr}(d,p)^{89}\text{Sr}$

the Coulomb displacement from Ref. [9]. The  $\alpha$  parameters, according to our purpose, had to obey the mass dependence from Fig. 1.

The criterion applied to select from a large number of «candidate» targets was the isotopic abundance. We have identified, on the basis of this criterion, more than twenty  $(d,p)$  reactions on nuclear targets starting with  $^{107}\text{Ag}$  up to  $^{130}\text{Te}$  target nuclei [21–33]. All these nuclei do exhibit the  $1/2$  spin orbit component of  $3p$  neutron strength function of significant intensity.

To get a global picture for the entire investigated mass region, as well as for a comparison with threshold anomaly reported for  $A \sim 90$  mass region, the same figure represents most of the predicted anomal cross sections (multiplied by corresponding scale factors) together with the largest experimental threshold anomalies measured for  $^{88}\text{Sr}(d,p)^{89}\text{Sr}$  [34] and  $^{94}\text{Zr}(d,p)^{95}\text{Zr}$  [35] stripping reactions (see Fig. 4). The experimental NSF for  $^{89}\text{Sr}$  and  $^{95}\text{Zr}$  residual target nuclei did reproduce better the threshold anomaly while multiplying  $\alpha$  parameters by the corresponding spectroscopic factors.

The predicted anomaly strengths  $\Delta'$  have also been calculated and represented, as scaled values in respect to the strongest anomal effect from  $^{88}\text{Sr}(d,p)^{89}\text{Sr}$ , versus mass number in Fig. 5. The stripping reactions under study were the following ones:  $^{107}\text{Ag}(1/2^-)(d,p)^{108}\text{Ag}(1^+)$ ,  $^{108}\text{Pd}(0^+)(d,p)^{109}\text{Pd}(5/2^+)$ ,  $^{109}\text{Ag}(1/2^-)(d,p)^{110}\text{Ag}(1^+)$ ,  $^{110}\text{Pd}(0^+)(d,p)^{111}\text{Pd}(5/2^+)$ ,  $^{110}\text{Cd}(0^+)(d,p)^{111}\text{Cd}(1/2^+)$ ,  $^{111}\text{Cd}(1/2^+)(d,p)^{112}\text{Cd}(0^+)$ ,  $^{112}\text{Cd}(0^+)(d,p)^{113}\text{Cd}(1/2^+)$ ,  $^{113}\text{Cd}(1/2^+)(d,p)^{114}\text{Cd}(0^+)$ ,  $^{114}\text{Cd}(0^+)(d,p)^{115}\text{Cd}(1/2^+)$ ,  $^{115}\text{I}(1/2^+)(d,p)^{116}\text{I}(1^+)$ ,  $^{116}\text{Sn}(0^+)(d,p)^{117}\text{Sn}(1/2^+)$ ,  $^{118}\text{Sn}(0^+)(d,p)^{119}\text{Sn}(1/2^+)$ ,  $^{120}\text{Sn}(0^+)(d,p)^{121}\text{Sn}(3/2^+)$ ,  $^{126}\text{Te}(0^+)(d,p)^{127}\text{Te}(3/2^+)$ ,  $^{128}\text{Te}(0^+)(d,p)^{129}\text{Te}(3/2^+)$ ,  $^{129}\text{Xe}(1/2^+)(d,p)^{130}\text{Xe}(0^+)$ ,  $^{130}\text{Te}(0^+)(d,p)^{131}\text{Te}(3/2^+)$ .

One should remark that the predicted threshold effects with  $A \sim 110$  target nuclei are much smaller (at least a factor of 5) or even indiscernible if compared to those with  $A \sim 90$  mass target nuclei.

## CONCLUSIONS

The inhibition of deuteron-stripping threshold anomaly related to  $p_{1/2}$  neutron single-particle state was explained both in terms of the direct interaction process and on the properties of the  $3p_{1/2}$  neutron threshold resonance.

Three factors have been found to be related with the DI process: (a) the  $Q$ -value dependence on  $(d, p)$  deuteron-stripping reaction, (b) the quantum kinematics involved in the DI transition amplitude, and (c) the spectroscopic factors of the residual nuclear state. Two of them, (a), (b), originate from the kinematics of the reaction while the third one, (c), depends on direct interaction dynamics.

The empirical relation between  $Q$  value of  $(d, p)$  reaction and the deuteron threshold energy has been successfully verified on the basis of experimental evidences for the  $A \sim 110$  mass region. The deuteron energy corresponding to neutron analogue channel is far away from the stripping cross-section peak for many of the candidate  $(d, p)$  reactions.

The quantum kinematics is determined by the transferred angular momenta and consequently, on the nuclear shell configuration of the residual and target nuclei of the stripping reaction. For both the  $d_{5/2}$  and the  $s_{1/2}$  transfer, the  $j_p = 3/2$  proton channel is favoured in displaying the anomalous effect, due to the interplay of Racah coefficients entering the transition amplitude element. Also the proton  $p$ -wave radial integrals are slightly larger for  $j_p = 3/2$  than for  $j_p = 1/2$  angular momenta.

Small spectroscopic factors of the involved residual states could reflect the incidence of multistep processes in the reaction mechanism. Their interference with one-step direct process will result in significant changes of magnitude of cross section that may mask small structures as threshold effects ones, superposed on the background excitation functions.

The two factors related to the  $3p$  neutron single-particle resonance may be classified following the above description, on their dependence on kinematical or dynamical aspects. The kinematical one is given by the energetic position of the  $j_p = 1/2$  single-particle resonance which may inhibit the magnitude of Lane resonant term for positive energy values. The second factor has a dynamical origin; on the basis of numerical calculations it was found that the compression of the energetic scale is about  $\sim 10\%$  weaker for  $j_p = 1/2$  single-particle resonance in respect of  $j_p = 3/2$  one.

The  $3p$  NSF contribution to deuteron-stripping threshold anomalies is modulated by a series of kinematical and dynamical factors as mentioned above. These factors do not contribute to evince better the  $3p_{1/2}$ -wave anomaly but rather they mask or even inhibit this threshold effect. However, one can consider some candidates for the threshold effects for  $A \geq 110$  mass target nuclei ( $^{107}\text{Ag}$ ,  $^{110-114}\text{Cd}$ ,  $^{116}\text{Sn}$ ,  $^{129}\text{Xe}$ ) even they are a factor of 5–10 smaller than those of  $A \sim 90$  target nuclei.

#### REFERENCES

1. *Hategan C., Graw G., Comisel H.* // Mod. Phys. Lett. 2005. V. 20. P. 187.
2. *Comisel H., Hategan C.* // Part. Nucl., Lett. 2003. No. [117]. P. 71.
3. *Comisel H., Hategan C.* // Mod. Phys. Lett. 2002. V. 17. P. 1315.
4. *Lane A. M.* // Phys. Lett. B. 1970. V. 33. P. 274.
5. *Samosvat G. S.* // Sov. J. Part. Nucl. 1986. V. 17. P. 313.
6. *Samosvat G. S.* // Part. Nucl. 1995. V. 26. P. 655.
7. *Stach W. et al.* // Nucl. Phys. A. 1979. V. 332. P. 144.

8. *Coker W. R. et al. // Phys. Rev. C. 1971. V. 4. P. 836.*
9. *Long D. D. et al. // Phys. Rev. 1966. V. 149.*
10. *Satchler G. R. Direct Nuclear Reactions. Oxford University Press, 1983.*
11. *Satchler G. R. // Nucl. Phys. 1964. V. 55. P. 1.*
12. *Yule T. J., Haeberli W. // Phys. Rev. Lett. 1967. V. 19. P. 756.*
13. *Lane A. M., Thomas R. G. // Rev. Mod. Phys. 1958. V. 30. P. 257.*
14. *Lynn J. E. The Theory of Neutron Resonance Reactions. Oxford Clarendon Press, 1968.*
15. *Ata M. S. et al. // Rom. J. Phys. (submitted).*
16. *Kunz P. D. The DWBA Code DWUCK. Private communication.*
17. *Ata M. S. et al. // Rom. J. Phys. 2002. V. 47. P. 709.*
18. *Becchetti F. D., Jr., Greenlees G. W. // Phys. Rev. 1969. V. 182. P. 1190.*
19. *Perey F. G. // Phys. Rev. 1963. V. 131. P. 745.*
20. *Lohr J. M., Haeberli W. // Nucl. Phys. A. 1974. V. 232. P. 381.*
21. *Brient C. E. et al. // Phys. Rev. C. 1972. V. 6. P. 1837.*
22. *Cohen B. I., Moorhead J. B., Moyer R. A. // Phys. Rev. 1967. V. 161. P. 1257.*
23. *Mlekodaj R. L. Thesis. Florida State University, 1973; Diss. Abst. Int. 1974. V. 34B. P. 5124.*
24. *Rosner B. // Phys. Rev. 1964. V. 136. P. 664.*
25. *Barnes P. D., Comfort J. R., Bockelman C. K. // Phys. Rev. 1967. V. 155. P. 1319.*
26. *Goldman L. H., Kremenek J., Hinds S. // Phys. Rev. 1969. V. 179. P. 1172.*
27. *Comfort R., Bockelman C. K., Barnes P. D. // Phys. Rev. 1967. V. 157. P. 1065.*
28. *Carson P. L., McIntyre L. C., Jr. // Nucl. Phys. A. 1972. V. 198. P. 289.*
29. *Schneid E. J., Prakash A., Cohen B. L. // Phys. Rev. 1967. V. 156. P. 1316.*
30. *Graue A. et al. // Nucl. Phys. A. 1968. V. 120. P. 493.*
31. *Moore W. H. // Nucl. Phys. A. 1967. V. 104. P. 327.*
32. *Graue A. et al. // Ibid. V. 103. P. 209.*
33. *Stroemich A. et al. // Phys. Rev. C. 1977. V. 16. P. 2193.*
34. *Zaidi S. A. A., Coker W. R., Martin D. G. // Phys. Rev. C. 1970. V. 2. P. 1384.*
35. *Heffner R. et al. // Phys. Lett. B. 1968. V. 26. P. 150.*